INTECH
open science | open minds

OPEN ACCESS
ARTICLE

International Journal of Advanced Robotic Systems

Preliminary Evaluation of Intelligent Intention Estimation Algorithms for an Actuated Lower-Limb Exoskeleton

Regular Paper

Mervin Chandrapal[1,*], XiaoQi Chen[1], Wenhui Wang[2], Benjamin Stanke[3] and Nicolas Le Pape[4]

1 Department of Mechanical Engineering, University of Canterbury, Christchurch, New Zealand.
2 Department of Precision Instruments, Tsinghua University, Beijing, China
3 School of Biomimetics, University of Applied Sciences, Factorial 5: Nature and Engineering, Bremen, Germany
4 Ecole Nationale Supérieure d'Ingénieurs de Limoges, Parc ESTER Technopole, Limoges, France
* Corresponding author E-mail: mervin.chandrapal@live.com

Received 18 Jan 2013; Accepted 5 Feb 2013

DOI: 10.5772/56063

Abstract This paper describes the experimental testing of an actuated lower-limb exoskeleton. The exoskeleton is designed to alleviate the loading at the knee joint by supplying assistive torque. It is hypothesized that the support provided will reduce the muscular effort required to perform activities of daily living and thus facilitate the execution of these movements by those who previously had limited mobility. The exoskeleton is actuated by four pneumatic artificial muscles, each providing 150N of pulling force to assist in the flexion and extension of the knee joint. The exoskeleton system estimates the user's intended motion using muscle activity information recorded from five thigh muscles, together with the knee angle. To experimentally evaluate the performance of the device, the exoskeleton was worn by an able-bodied user, whilst performing the sit-to-stand-to-sit movement. In addition, the three intention estimation algorithms were also tested to determine the influence of the various algorithms on the support provided. The results show a significant reduction in the user's muscle activity (≈ 20%) when assisted by the exoskeleton in a predictable manner.

Keywords EMG-to-Force, Exoskeleton, Artificial Neural Networks, Differential Evolution

1. Introduction

Research on exoskeleton devices to augment or support a human user is not a new idea. Human imagination and science fiction has made popular the notion that a wearable mechanical device could allow the human operator to push physical boundaries. However, the realization of these devices has only been possible in the modern era, with the advent of the computer, compact actuators and power storage capabilities. Dollar et al. [1] state that focused research on exoskeletons only began in the late 1960s in both the United States of America and the former Yugoslavia [2]. Whilst research in the USA was mainly driven by the military, the goal of the latter was to help patients with defects in the locomotor system to regain mobility. Since those early years, exoskeleton research has grown to encompass a much larger field of application. In addition to the original military and medical applications, exoskeletons are also currently being developed to assist in rehabilitation, to support factory workers while performing manual work, to increase the mobility of the elderly and even for purely entertainment purposes.

In the context of this work, an exoskeleton is defined as a mechanical device worn in permanent or close contact with a human operator. The device is essentially anthropomorphic in nature, with flexibility and intelligence to work in concert with the operator's movements [3]. Exoskeletons can be broadly grouped into three categories: rehabilitation exoskeletons, mobile medical exoskeletons and performance-augmenting exoskeletons [4]. Medical exoskeletons are assistive and/or rehabilitative devices that are portable and can be used in a non-clinical setting. In contrast to performance-augmenting exoskeletons, these are designed to be worn by a person with limited mobility due to age or gait disability. Unlike rehabilitation exoskeletons, medical exoskeletons presuppose the patient's ability to maintain postural stability. The fundamental purpose of this type of exoskeleton is to compensate the lack of force in the joint (or joints) and support the user's body weight so as to minimize the loading on the joint [4].

The most popular medical exoskeleton is the hybrid assistive limb (HAL) series, developed at the University of Tsukuba [5–7]. The commercial device was initially built as a lower body exoskeleton, but was later extended to encompass the whole body. The primary purpose of the device was to improve the mobility of the elderly and to support patients suffering from degenerated muscles, spinal cord injury or brain injury, during activities of daily living (ADLs). The modularized, lower-limb exoskeleton incorporated six DC motors with harmonic drives to actuate the hip, knee and ankle joint on both legs, about the sagittal plane. Public demonstrations of the device show an able-bodied user easily lifting weights of up to 40kg.

The wearable walking helper (WWH) designed at Tohuku University is another lower-limb medical exoskeleton [8, 9]. Similar to the HAL, the WWH was aimed specifically at those who are physically weak and unable to support their body weight for a sustained period. The authors stated that the design of the exoskeletons was inspired by passive support mechanism such as canes, caster walkers and walking frames. These passive devices do not just increase stability, but also partly reduce the loading, due to gravitational forces, on the muscles. The WWH exoskeleton presupposes that the user is able to determine and maintain a stable posture. The device only alleviates the loading and reduces the strenuousness of the movement.

More recently, there has been renewed research into lower-limb exoskeletons designed to provide gait assistance to paraplegics and hemiplegics [10, 11]. The operation of these devices defers slightly from the other medical exoskeletons in that the exoskeleton not only provides assistive torque at the joints, but also directs the movements of the user's limbs. Stringent limits are generally imposed to the user's gait to ensure that the ideal joint trajectory, for a particular ADL, is adhered to.

Exoskeleton development has a substantial advantage over general robot development because exoskeletons can rely on the intelligence of the human user. By tapping into the human user, the exoskeleton can take advantage of all the sensors, computational power, control system, and mechanics that the human possesses. As a result, the types of controllers that need to be designed for exoskeletons are quite different from the types of controllers that are designed for autonomous independent robots [12]. In the HAL series, a hybrid control architecture that utilized both a state machine and skeletal muscle activity was implemented. The user's intention was estimated from the magnitude of the muscle activation, and used to transition from one ADL to another.

The use of both biological and kinematic information to estimate the intended motion has several advantages. This type of intention estimation algorithm is inherently flexible and generally allows fluent, arbitrary transitions between movements. The biological signals from the muscles, acquired through electromyography, allow the device to form a close bond with the human user and estimate the intended movement even before it is produced. On the other hand, this integration comes with several drawbacks. The union of the exoskeleton with the human user will only be successful if the exoskeleton functions in cooperation with the physiology and biomechanics of the human body. This is severely limiting because the biomechanics of human movement is not yet thoroughly understood [13]. Currently, it still is not clear how gait pattern affects the metabolic cost during walking. If this relation has not been identified, then naturally it will be difficult to design an exoskeleton control system to optimize the metabolic cost. Nevertheless, the study of human gait when assisted by an exoskeleton can provide new insights into human locomotion.

This paper describes an actuated lower-limb exoskeleton that is intended to provide gait assistance to a user by supplying assistive torque at the knee joint during dynamic ADLs. The torque provided is intended to reduce the muscular effort required to perform ADLs. Based on the previous definition given, the exoskeleton described here could be classified as a medical exoskeleton for the lower-limb. In this work, only the sit-to-stand-to-sit (STS) movement is analysed, as it is known to be the movement that requires the most effort and where the torque is particularly high at the knee joint. Thus, the effect of the added torque from the exoskeleton should be evident during this movement. The experiments described in this paper attempt to analyse two key factors regarding powered assistance:

1. Does the assistive torque supplied by the exoskeleton to the user manage to reduce the muscular effort required to perform the STS movement?
2. Does the method used to estimate the user's intended movement affect the fluency and effectiveness of the assistive torque?

This paper is organized as follows: in Section 2 the hardware and software components of the prototype exoskeleton system are presented. The experimental procedure is explained in Section 3. The results of the STS experiments are presented and discussed in Section 4. Finally, the findings are summarized and the paper is concluded in Section 5.

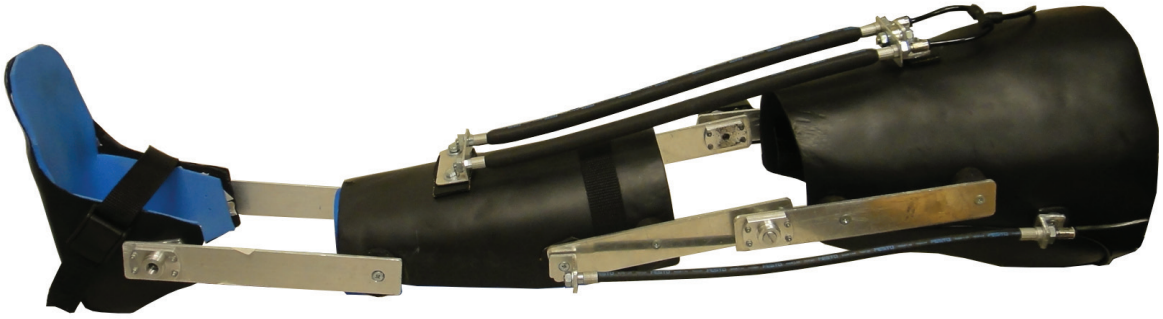

Figure 1. Complete leg brace with PAMs and sensors.

2. Pneumatic lower-limb exoskeleton

The actuated lower-limb exoskeleton prototype that was constructed is shown in Figure 1. The exoskeleton was custom fabricated from carbon fibre to fit snugly on the test subject. The device provides assistive torque for extension[1] and flexion[2] about the sagittal plane at the knee joint. The ankle joint is unactuated and left passive. Currently, only a single device on the right leg is utilized to provide support to the user. The actuation of the knee joint is realized using four pneumatic artificial muscles (PAM), two for flexion and two for extension. The PAMs have a high power to weight ratio and are inherently compliant [14, 15]. Each PAM is capable of generating a maximum pulling force of 150N. The flexor and extensor PAMs are 300mm and 400mm long, respectively. The use of these actuators, particularly for anthropomorphic applications, has drawn much interest over the past decade [16, 17] due to their skeletal muscle-like characteristics.

The nonlinear control algorithm developed to compensate for the nonlinearities inherent in the actuator have been described in detail in [18]. Briefly, an adaptive fuzzy controller that iteratively improves the control output has been implemented. The controller uses the error signal that is calculated based on the torque feedback to adapt to the plant and improve the control action. Two load cells attached in series to the actuators provide the feedback to the motion control loop. The control output varies the pressure within the PAMs through a proportional pressure regulator (PPR) and a pair of high speed valves (HSV). The PPR regulates the pressure in the extensor PAMs and the HSVs regulate the pressure within the flexor PAMs. A rotary encoder embedded into the knee joint provides position feedback of the knee angle. The convention used for the knee angle in the exoskeleton is 0° when the leg is fully extended, with the angle increasing in the positive direction as the knee is flexed. The mechanical properties of the exoskeleton are summarized in Table 1.

	DOF	ROM (degrees)	Torque (Nm)
Hip	N/A	N/A	N/A
Knee	1	110/0[1]	15/35[1 2]
Ankle	1	50/20[1]	Unactuated

[1] Joint Flexion/Extension
[2] Maximum torque values

Table 1. Mechanical properties of the lower-limb exoskeleton.

[1] Movement of the lower leg away from the back of the thigh.
[2] Movement of the lower leg towards the back of the thigh.

2.1. Electromyography

The computation of the support provided by the exoskeleton is performed by the intention estimation algorithm. The algorithm estimates the actual torque at the knee joint based on the muscle activation signals and the knee joint angle. The use of muscle activation signals acquired through surface electromyography (sEMG) provides a direct link to the desired motion (even unconscious motion), by analysing the contraction of the related muscles. The movement of the limb or joint is not strictly necessary. Even if the muscles are too weak or the external load is too heavy, the intention (i.e., sEMG signal) can still be detected. Furthermore, a conscious effort is not necessary to produce or maintain the sEMG signal, and this activation signal can be detected 2080ms prior to muscle contraction, reducing the latency of the intention estimation algorithm.

The user's muscle activity or myoelectric signals are recorded through five pairs of non-invasive sEMG sensors placed on the skin surface above the muscle of interest. The reusable, active, bipolar electrodes were constructed with a built in pre-amplifier circuit, that amplifies the detected signals 4000 times (Figure 2). The dimension (circular electrodes, 10mm diameter in the direction of the muscle fibre) and the inter-electrode distance (20mm) were fixed based on SENIAM[3] recommendations [19]. In this work, sEMG data from **five** major muscles that flex and extend the knee were recorded for the exoskeleton intention estimation algorithm. The muscles that were monitored are the *rectus femoris* (RF), *vastus medialis* (VM), *vastus lateralis* (VL), *biceps femoris* (BF) and *semitendinosus* (ST). In total, these muscles cover approximately 63% of the thigh cross-sectional area. The smaller muscles of negligible cross-sectional area and muscles that are also involved in flexing the hip or the ankle are not evaluated for the intention estimation algorithm. Prior to placement, the electrodes were gelled and the placement site was shaved and cleaned with alcohol to reduce surface impedance. During reattachment on subsequent days, care was taken (visually) to ensure that the electrodes were placed at the same site. The electrodes were placed proximal to the midpoint of each muscle belly, to avoid the innervation zones and to reduce cross talk [20]. Guidelines provided by [21] were used as reference for electrode

[3] The SENIAM project (Surface ElectroMyoGraphy for the Non-Invasive Assessment of Muscles) is a European concerted action in the Biomedical Health and Research Program (BIOMED II) of the European Union.

placement. The reference (ground) electrode was attached on the front of the tibia on the same (right) leg.

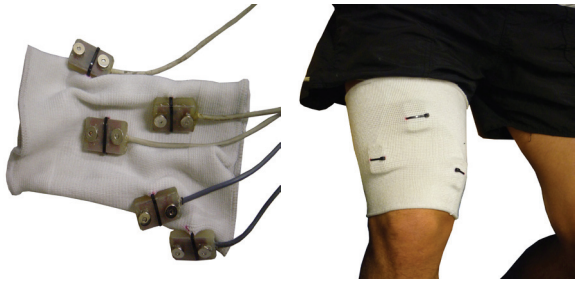

(a) (b)

Figure 2. (a) Surface electrodes attached to an elastic thigh band to minimize movement. (b) Position of extensor electrodes when worn by the user.

All five pre-amplified sEMG signals were sampled simultaneously at 2kHz. Based on recent research, the sEMG signals were then band-pass filtered at approximately 400600Hz using a 2^{nd} order Butterworth filter [22, 23]. The signals were then rectified and low pass filtered (1.5Hz-2^{nd} Order Butterworth filter) to obtain the activation envelope. The low pass filtering replicates the 2^{nd} order muscle twitch response to the impulse from the motor unit action potential [24].

The sEMG data were then normalized to provide a common basis of comparison across different sessions and different muscles. Normalization expresses all other muscle activity as a percentage of a base or anchor point. The most common anchor point used is the *maximum voluntary isometric contraction*[4] (MVIC). The instantaneous amplitudes are presented as a percentage of the highest sEMG amplitude in a MVIC. In order to obtain a better approximation of the MVIC at different knee angles, MVIC tests were carried out at seven knee angles on an isometric test rig. The seven values are then used to normalize the data acquired during the dynamic ADL movement. Linear interpolation was used to obtain MVIC values for intermediate knee angles. The justification of this normalization method is based on previous work and is detailed in [25].

2.2. Force and position sensors

Data from the encoder, load cells and sEMG sensors were acquired and processed using a National Instruments (NI) cRIO real-time controller. The NI 9401 module is used to read the encoder outputs and to control the HSVs. The two load cells were sampled at 100Hz in full bridge mode using the NI 9219 module. All five sEMG sensors were sampled at 2kHz in parallel, with the NI 9205 module. Finally, the PPR was controlled with the voltage output from the NI 9263 module. An overview of the hardware structure of the control system and the flow of data is illustrated in Figure 3, and a list of the hardware used in the exoskeleton is given in Table 2.

[4] Muscular contraction against resistance without movement such that the length of the muscle does not change, i.e., constant joint angle

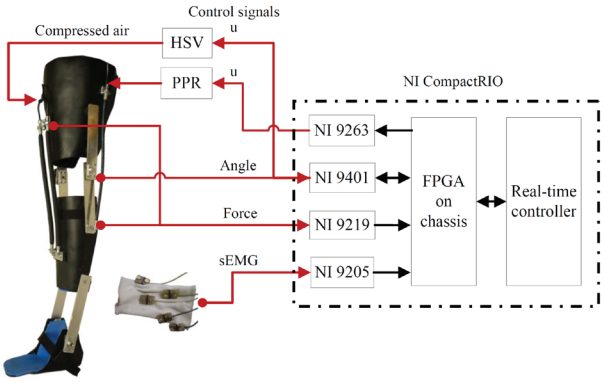

Figure 3. Exoskeleton hardware structure and data flow. The black arrows indicate the data flow within the cRIO. The red arrows indicate the external data flow from and to the real-time controller.

2.3. Exoskeleton control algorithm

The support provided by the exoskeleton is correlated to the torque exerted by the user at the knee joint. An intention estimation algorithm was introduced to estimate the magnitude and direction of the actual torque (from the user's muscle) at the knee joint based on the instantaneous sEMG (processed and normalized) and joint angle data. The exoskeleton control architecture is illustrated in Figure 4. This intention estimation algorithm was built offline and then incorporated into the exoskeleton system. To obtain a feasible mapping of the six input parameters (i.e., sEMG from five muscles and knee angle) to the resultant joint torque, intelligent machine learning algorithms were employed.

The procedure used to develop the algorithms is visualized in Figure 5. The basis of this algorithm is to use sEMG-to-knee joint torque characteristics obtained during isometric tasks, and extend it to dynamic motion by including dynamic muscle characteristics. Previous attempts have proven that intelligent algorithms are capable of estimating isometric torque with high accuracy using very few free parameters [25]. In this work, this advantage is exploited to estimate dynamic torque by incorporating additional muscle force-length characteristics, obtained through the knee angle.

While the predefined isometric tasks were performed, sEMG data from the five knee muscles were recorded together with the joint torque and the knee angle. The isometric tests were carried out at various knee angles (on the sagittal plane) to incorporate force-length characteristics. Next, the sEMG data was processed and normalized as usual. The normalized sEMG, torque and

Real-time platform	NI cRIO 9022
NI modules	9401, 9219, 9205, 9263
PAM	FESTO DMSP-5-300 & 400
PPR	FESTO MPPES-3-1/8-6-010
HSV	FESTO MHE2-MS1H-3/2G)
Position feedback	US digital S5-360
Force feedback	2×LCM201-200N
sEMG sensors	5×Own construction

Table 2. List of equipment used for the exoskeleton system.

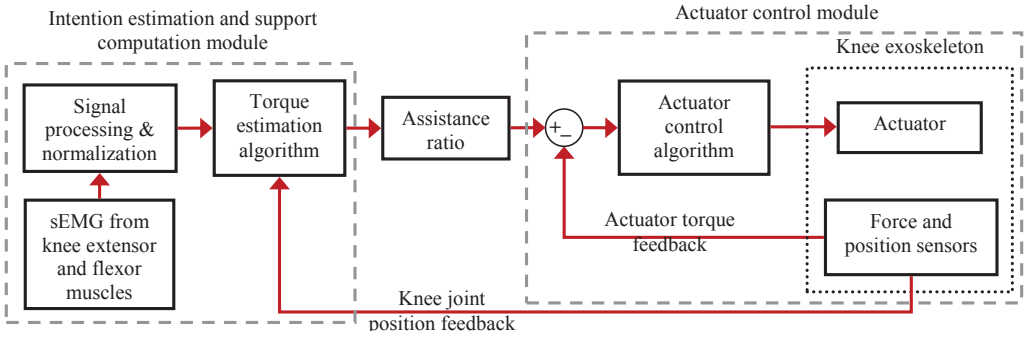

Figure 4. Control block diagram of the knee exoskeleton. The exoskeleton system consists of two main modules, the intention estimation module and the actuator control module.

knee angle data were then utilized to train and validate the intelligent mapping algorithms.

Three different forms of intelligent intention estimation algorithms were implemented to provide a comparison and to determine the better algorithm for the exoskeleton. The first form utilized an artificial neural network (ANN), similar to that employed for estimating elbow joint torque [26]. ANNs, initially inspired by biological information processing, have proven to be excellent tools for nonlinear function approximation. The multilayer perceptron (MLP) architecture with three layers (input → hidden → output) is the most common ANN implemented. The MLP model used in this work was implemented using MATLAB's Neural Network Toolbox and is illustrated in Figure 6. The first layer consists of six independent variables (normalized sEMG from five muscles and the knee angle (γ) in radians). The second layer (also known as the hidden layer) contains a variable number of hidden nodes (neurons) that represent the ANN's learning and knowledge storage capacity. The third layer contains a single output node representing the estimated knee joint torque. The MLP network was trained iteratively using the recorded isometric data until either the gradient was sufficiently small (less than 1×10^{-5}), the number of epochs exceeded 1000 or the generalization error (used as an early stopping criterion) started to increase indicating that overfitting had occurred.

The second and third intention estimation algorithms utilized an evolutionary optimization approach, based on the differential evolution algorithm. A survey of past research has shown that both linear [27] and nonlinear (parabolic) [23, 28] algebraic functions have been successfully adapted to describe the sEMG to muscle force

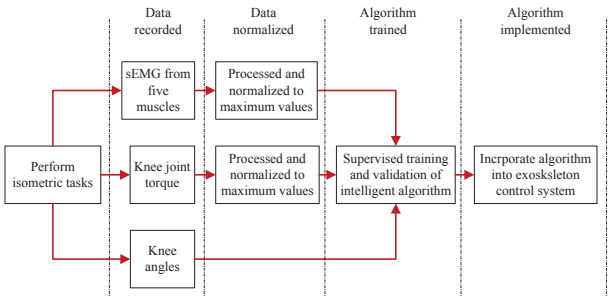

Figure 5. The processes involved in developing a sEMG to torque mapping algorithm, using isometric data, for the exoskeleton.

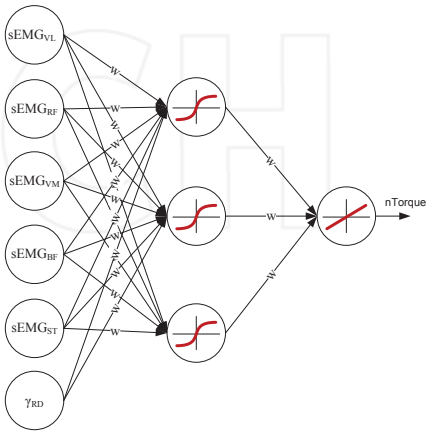

Figure 6. Example of a multilayer perceptron (MLP) network with three neurons in the hidden layer, used for knee torque estimation. The inputs are the normalized sEMG from the five muscles and the knee angle (in radians). The respective activation functions at each neuron and the individual synaptic weights (w) are shown.

relationship in isometric contractions. This success was extended here to estimate dynamic torque, in the same way as the MLP algorithm. The incorporation of the knee angle as an additional variable in the equation provided the necessary force-length information. The equation used for the linear mapping is given by:

$$\begin{aligned} nTorque = {} & x_1(sEMG_{VL}) + x_2(sEMG_{RF}) \\ & + x_3(sEMG_{VM}) + x_4(-sEMG_{BF}) \\ & + x_5(-sEMG_{ST}) + x_6(\gamma_{RD}) \end{aligned} \quad (1)$$

where the total torque at the knee joint is the linear summation of the individual, normalized sEMG amplitudes, $sEMG_{xx}$, and the knee angle, γ_{RD}. The coefficients $x_{1\to6}$ are the scaling factors of the independent variables. The sign convention used in the estimation algorithms is positive for knee extension torque and negative for flexion torque. Accordingly, the flexor muscles (BF and ST) were weighted negative as they contribute to the negative knee torque. The equation for the nonlinear mapping follows a similar pattern, where each of the six independent variables was represented by an exponential function (Equation 2). The basic form of the function is adapted from the works of [23, 29, 30].

$$
\begin{aligned}
nTorque = & \frac{e^{(-0.001\times sEMG_{VL}\times x_1)}-1}{e^{(-0.1\times x_1)}-1} \\
& + \frac{e^{(-0.001\times sEMG_{RF}\times x_2)}-1}{e^{(-0.1\times x_2)}-1} \\
& + \frac{e^{(-0.001\times sEMG_{VM}\times x_3)}-1}{e^{(-0.1\times x_3)}-1} \\
& + \frac{e^{(-0.001\times sEMG_{BF}\times x_4)}-1}{e^{(-0.1\times x_4)}-1} \\
& + \frac{e^{(-0.001\times sEMG_{ST}\times x_5)}-1}{e^{(-0.1\times x_5)}-1} \\
& + \frac{e^{(-0.001\times \gamma_{RD}\times x_6)}-1}{e^{(-0.1\times x_6)}-1}
\end{aligned} \tag{2}
$$

In both the linear and nonlinear equations there are six coefficients that determine the contributions of the independent variables to the resultant joint torque. To find the optimal values for all the coefficients, the differential evolution optimization algorithm was employed. Differential evolution (DE) is a type of evolutionary algorithm that applies the principles of biological evolution to mathematical problems, to minimize a cost function over the course of successive generations [31]. Similar to other evolutionary algorithms, DE solves optimization problems by first generating a population, then evolving the candidates through a crossover and mutation operation. The next generation of candidates are chosen based on the best fitness value (lowest cost) of the evolved current population. Various implementations have proven DE to be an excellent global optimization algorithm for continuous numerical minimization problems. A comprehensive explanation of the DE algorithm is given in [32].

Finally, the calibrated intention estimation algorithm (MLP, DE-Linear or DE-Exponential) is incorporated into the exoskeleton control loop to estimate the resultant torque acting at the user's knee joint during dynamic ADL movements. A positive estimated torque indicates knee extension and a negative torque indicates knee flexion. As shown in Figure 4, the estimated torque is then scaled using an assistance ratio (AR) which varies the magnitude of the assistive torque added by the exoskeleton.

3. Experimental procedure

In order to experimentally validate the ability of the exoskeleton to provide assistive torque, the previously described exoskeleton was worn and tested by an able-bodied user. In addition, the experiments also evaluated the robustness and reliability of the three intention estimation algorithms. The experiments were carried out with one subject (physically healthy, 26-year-old male, weight: 66kg, height: 1.74m), on 10 random days, over a period of three weeks to incorporate inter and intra-session variation. The test procedure was explained to the subject and written consent was obtained prior to participation.

3.1. Calibration

On each of the 10 days, the user was first required to complete a single isometric contraction session on an isometric apparatus. The single session consisted of maximal isometric extension and flexion at seven knee angles ($0°, 15°, 30°, 45°, 60°, 75°, 90°$). During the isometric contractions, joint torque, sEMG and knee angle data were collected and processed (see Section 2.1 - electromyography). Then, the data were used to train the MLP network and to determine the coefficients of the linear and exponential estimation functions.

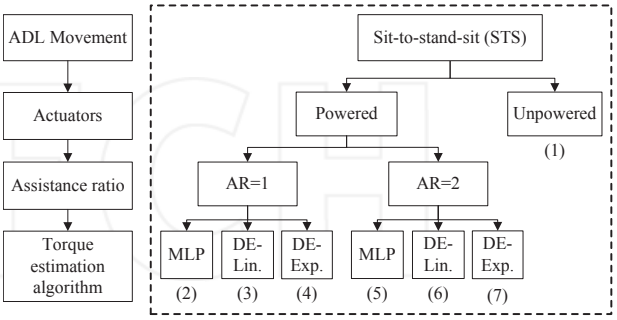

Figure 7. The numbers denote the seven categories (and the order) assessed with the final exoskeleton system. The assistance ratio (AR) is used to scale the estimated torque.

3.2. Protocol

After this calibration step, the user, wearing the exoskeleton, performed the STS movement. To clarify the experimental procedure, the seven assessment categories are illustrated in a flowchart in Figure 7. The procedure allowed a thorough evaluation of the different factors that would affect the exoskeleton system. The subject was instructed to execute 10 repetitions (for each category) of the complete STS movement, whilst seated on a chair that was adjusted to a comfortable height. The STS movement was performed at a slow pace without any external support from arm rests to mimic the movements of a user who would require assistance. The position of the legs and the arms were kept constant throughout the experiments to standardize the movement.

3.3. Lower-limb kinematics

During the experiments, joint angle information was recorded from the encoder at the knee joint. The knee angle data were used to objectively evaluate the smoothness and predictability of the motion. The number of inflection points in a powered STS movement was compared to that from an unpowered movement. The difference was expressed as a percentage variation and gave an estimate of the exoskeleton's effect on the gait. This approach was chosen as it provided a statistical comparison of the data rather than simply comparing the knee angle visually.

3.4. Surface electromyography

The sEMG from the knee extensors and flexors, which were used for the torque estimation algorithms, were also

recorded to observe muscle activity. The change in muscle activity levels, as measured through the normalized sEMG signals, indicated whether the exoskeleton assisted or obstructed the movement. The peaks in each sEMG recording, above a certain threshold, were detected and averaged, after the outliers were removed. These mean values represented the maximum muscle activity in each category for the STS movement. The variation between the mean values for powered movement and unpowered movements were represented as a percentage. If the resulting percentage has a negative sign, then the powered exoskeleton has managed to reduce the muscle activity. Conversely, if the sign is positive, then the muscle activity has increased due to the external torque from the exoskeleton.

3.5. Metabolic cost

In addition, metabolic data were collected simultaneously for all experiments to determine the change in metabolic cost as a result of the assistive torque. The COSMED K4b^2 portable metabolic measurement system (COSMED s.r.l., Rome, Italy) was used for this purpose. The lightweight, battery operated, wireless and self-contained device, measured oxygen consumption ($\dot{V}O_2$) and carbon dioxide production ($\dot{V}CO_2$) on a breath-by-breath basis. $\dot{V}O_2$ is one of the most fundamental and widely recognized measures of energy consumption as defined by two key components: the delivery of oxygen to skeletal muscle and the ability of the muscle to extract and use O_2 [33]. In each of the experiments, the breath-by-breath values for the $\dot{V}O_2$ (ml/min) and $\dot{V}CO_2$ (ml/min) were used to calculate the energy expenditure (EE) per hour (kJh^{-1}) using the equation described in [34]. The EE values were first averaged over a 15 second period and then over the entire STS movement. Finally, similar to the sEMG data, the EE values were expressed as percentage variations from the unpowered STS movements, which were used as baseline EE values.

Over the course of the 10 days, 100 complete STS movements were processed and analysed. The final results (in percentage variation) of the knee angle, sEMG data and metabolic data were averaged over the 10 days, to minimize error.

4. Results and Discussion

The results of the experiments for each ADL motion were considered from both a subjective and objective perspective. Subjective feedback was obtained verbally from the user during the experiments. These results gave an indication of the exoskeleton's comfort, predictability and reliability as perceived by the user. These results are just as important as the objective data, because if the user did not have confidence in the system, then he would be apprehensive when using the device. The objective results were based on the recorded knee angle, normalized sEMG and metabolic rate.

The STS movement is generally recognized as one that requires the largest torque at the knee joint. An assistive exoskeleton could definitely supplement the large torques required to complete the motion. However, due to the large torques involved, extra caution was necessary to prevent unnatural forces.

	Assist. Ratio	Knee angle	EE
Unpowered	0	0.00	0.00
MLP	1	8.33	8.69
	2	17.67	8.72
DE-Lin.	1	3.43	2.93
	2	4.65	10.43
DE-Exp.	1	8.73	12.32
	2	25.30	11.45

Table 3. Mean difference in knee angle and EE for STS movement (%)

During the experiments with the MLP algorithm (AR=1), the user felt comfortable and confident in the exoskeleton. The user could feel the positive assistive torque during the sit-to-stand phase. The exoskeleton did not obstruct the movement and the motion was relatively smooth. This is attested by the knee angle data shown in Table 3. The peak sEMG values (Table 4) were also reduced for all extensor muscles and for one of the flexor muscles, implying that the user benefited from the added support. When the support was increased (AR=2), the movement became jerky and the user did not feel completely safe during the movement. The jerky motion is reflected in the knee angle data, which shows $\approx$ 17% variation in gait. Correspondingly, an increase in muscle activity to counteract the unpredictable assistance is observed in four muscles (Table 4). However, the increase in peak muscle activity is not as large as would be expected from such jerky motion. This very slight increase could be attributed to the user consciously transferring the load to the unsupported leg, to reduce the activity of the muscles and control the jerky motion.

According to the user, the STS motion performed with the DE-Linear algorithm was the most comfortable and predictable. The motion could be performed fluidly even when the AR was increased. The exoskeleton moved in unison with the user and no jerky motions were felt. The recorded knee angles for the linear algorithm have the smallest percentage variations, for both ARs, compared to the other two algorithms (Table 3). With the AR=1, there is negligible change in the peak sEMG for the extensor muscles, but a significant increase in flexor muscle activity (Table 4). When the AR was increased (AR=2), the results show a reduction in peak sEMG for all five muscles. The total reduction in muscle activity for the STS movement is the highest at this setting when compared to the other five categories. This indicates that this algorithm provided the best estimation of the user's intention for this movement.

The performance of the DE-Exponential algorithm is the worst of the three. At AR=1, the STS movement could be performed easily with slight perturbations. The user generally felt comfortable and had confidence in the device. However, the mean peak sEMG values reveal that the exoskeleton did not affect significant change to the extensor muscles' activity levels. Moreover, the flexor muscles show an increase in muscle activity. The increase of the AR resulted in erratic and unreliable support from the exoskeleton. It was extremely difficult for the user to perform the motion and considerable effort was required

not to transfer all the load onto the unsupported leg. The recorded knee angle shows a variation of ≈ 25% and an increase in muscle activity is evident in four of the knee muscles (Table 4).

	Assist. Ratio	VL	RF	VM	BF	ST
Unpowered	0	0	0	0	0	0
MLP	1	-16.60	-21.67	-9.77	49.29	-11.67
	2	13.21	4.32	13.05	59.82	-10.02
DE-Lin.	1	1.64	-5.10	2.68	17.80	17.71
	2	-18.80	-19.32	-13.72	-7.81	-14.69
DE-Exp.	1	4.29	-4.39	3.22	10.10	13.46
	2	14.81	-14.06	18.18	76.37	34.15

Table 4. Mean difference in peak sEMG for STS movement (%)

In almost all the experiments, it was noticed that the BF showed a substantial increase in muscle activity (up to 76%). After further investigation of the normalized sEMG pattern, it was discovered that this increase occurred during the stand-to-sit movement. During this phase, both the knee flexor and extensor muscle are activated to increase the stiffness of the joint and cushion the seating movement (eccentric contraction). However, the intention estimation algorithms implemented in this work are only capable of estimating either a positive (extensor) or a negative (flexor) torque. The co-contraction of the muscles usually resulted in the algorithms estimating a positive torque and consequently the extensor PAMs were contracted. The BF muscle therefore had to increase the flexion force to oppose this added positive torque.

The energy expenditure data recorded (Table 3) show that, in general, the assistive torque at the knee joint increased the metabolic cost. The DE-Linear estimation algorithm (at AR=1) resulted in the lowest increase ($\approx 3\%$), but from the corresponding sEMG data it is known that this category had little effect on the muscle activity. All the other five categories show an increase in EE of approximately 8% to 10%. The analysis of the energy expenditure in all the STS experiments shows an increase in the metabolic cost. When compared to the data from the muscle activation, the two seem contradictory. However, to better understand the results, it is important to consider the entire system, i.e., the human user and the exoskeleton. Since only one leg is assisted by the exoskeleton, the added torque on that leg could disrupt the naturally efficient gait symmetry during the STS movement. The uneven external torque applied to the human body during a synchronous motion may well be the cause of the increased EE.

Another important factor that follows from this is that an able-bodied user is capable of efficiently executing the STS movement without the exoskeleton. When assisted by the exoskeleton (on only one leg), this natural balance may be disrupted, causing an increase in EE. Nevertheless, it cannot be assumed that a similar scenario would occur when a person who needs the added assistance performs the same movement. In other words, the same assistive torque that increased the EE of an able-bodied user may in fact reduce the EE of a person with weak muscles. Further experiments on actual patients are necessary to confirm this.

5. Conclusion

The preliminary experimental results obtained for the exoskeleton system are presented in this paper. The influence of the assistive torque from the exoskeleton on an able-bodied user was tested for the STS movement, which requires high torques at the knee joint. The analysis of the exoskeleton's performance was based on both subjective feedback from the user and objective data recorded from the encoder, sEMG sensors and a portable metabolic measurement system. The experiments conducted have, to a certain degree, substantiated the claim that a powered lower-limb exoskeleton could reduce the muscular effort required to perform certain ADL movements. The results indicate that the exoskeleton is well suited to provide assistance to slow movements which require large torques. When the exoskeleton provides this additional torque in a predictable manner, the user has been shown to be able to accommodate this external support and reduce his muscle activity, while performing the desired movement.

When comparing the three intention estimation algorithms proposed, based on knee angle variation and reduction in sEMG, the MLP and DE-Linear algorithm both have comparable performance, while the DE-Exponential algorithm has the worst overall performance. However, based on both the subjective and objective data, the DE-Linear algorithm appears to be more robust and predictable for the STS movement. Moreover, since the parameters of the DE-Linear algorithm are more transparent than the MLP, it is possible to appreciate the contribution of individual flexor and extensor muscles to the total joint torque. Based on these factors, the DE-Linear algorithm is considered as the better algorithm.

6. Acknowledgements

The authors gratefully acknowledge Julian Murphy and Gavin Blackwell for their contributions to the research and experimental activity presented in this paper.

7. References

[1] A. M. Dollar and H. Herr. Lower extremity exoskeletons and active orthoses: Challenges and state-of-the-art. *IEEE Transactions on Robotics*, 24(1):144–158, 2008.

[2] M. Vukobratovic, D. Hristic, and Z. Stojiljkovic. Development of active anthropomorphic exoskeletons. *Medical & Biological Engineering*, 12(1):66–80, Jan 1974.

[3] Hugh Herr. Exoskeletons and orthoses: classification, design challenges and future directions. *Journal of Neuroengineering and Rehabilitation*, 6:21–30, 2009.

[4] K.H. Low. Robot-assisted gait rehabilitation: From exoskeletons to gait systems. In *Defense Science Research Conference and Expo (DSR)*, pages 1 –10, aug. 2011.

[5] H. Kawamoto, Suwoong Lee, S. Kanbe, and Y. Sankai. Power assist method for hal-3 using emg-based feedback controller. In *IEEE International Conference on Systems, Man and Cybernetics*, volume 2, pages 1648–1653, 2003.

[6] H. Kawamoto and Y. Sankai. Power assist method based on phase sequence driven by interaction between human and robot suit. In *IEEE International Workshop on Robot and Human Interactive Communication*, pages 491–496, 2004.

[7] S. Lee and Y. Sankai. The natural frequency-based power assist control for lower body with hal-3. In *IEEE International Conference on Systems, Man and Cybernetics*, volume 2, pages 1642–1647, 2003.

[8] T. Nakamura, K. Saito, ZhiDong Wang, and K. Kosuge. Realizing a posture-based wearable antigravity muscles support system for lower extremities. In *9th International Conference on Rehabilitation Robotics*, pages 273–276, 2005.

[9] T. Nakamura, K. Saito, Z. D. Wang, K. Kosuge, and M. Tajika. Human cooperative motion adapted wearable anti-gravity muscle support system. In *IEEE/RSJ International Conference on Intelligent Robots and Systems*, pages 1843–1848, 2006.

[10] H. Kawamoto, T. Hayashi, T. Sakurai, K. Eguchi, and Y. Sankai. Development of single leg version of hal for hemiplegia. In *Annual International Conference of the IEEE Engineering in Medicine and Biology Society*, pages 5038–5043, 2009.

[11] R. J. Farris, H. A. Quintero, and M. Goldfarb. Preliminary evaluation of a powered lower limb orthosis to aid walking in paraplegic individuals. *IEEE Journal on Neural Systems and Rehabilitation Engineering*, 19(6):652–659, 2011.

[12] Daniel P. Ferris. The exoskeletons are here. *Journal of Neuroengineering and Rehabilitation*, 6:17–20, 2009.

[13] Daniel P. Ferris, Gregory S. Sawicki, and Monica A. Daley. A physiologist's perspective on robotic exoskeletons for human locomotion. *International Journal of Human Resources*, 4(3):507–528, Sep 2007.

[14] Kanji Inoue. Rubbertuators and applications for robots. In *The 4th international symposium on Robotics Research*, pages 57–63, 1988.

[15] D. G. Caldwell, G. A. Medranocerda, and M. Goodwin. Control of pneumatic muscle actuators. *IEEE Control Systems Magazine*, 15(1):40–48, 1995.

[16] K. Balasubramanian and K. S. Rattan. Fuzzy logic control of a pneumatic muscle system using a linearizing control scheme. In *22nd International Conference of the North-American-Fuzzy-Information-Processing-Society (NAFIPS)*, pages 432–436. IEEE, 2003.

[17] Yong-Lae Park, Bor-rong Chen, Diana Young, Leia Stirling, Robert J. Wood, Eugene Goldfield, and Radhika Nagpal. Bio-inspired active soft orthotic device for ankle foot pathologies. In *IEEE/RSJ International Conference on Intelligent Robots and Systems*, pages 4488–4495, 2011.

[18] Mervin Chandrapal, XiaoQi Chen, Wenhui Wang, and Chris Hann. Nonparametric control algorithms for a pneumatic artificial muscle. *Expert Systems with Applications*, 39(10):8636Ű8644, 2012.

[19] Hermie J. Hermens, Bart Freriks, Roberto Merletti, Dick Stegeman, Joleen Blok, GÃijnter Rau, Cathy Disselhorst-Klug, and GÃűran HÃd'gg. *SENIAM 8 European Recommendations for Surface ElectroMyoGraphy, results of the SENIAM project*. Roessingh Research and Development b.v., 1999.

[20] C. J. De Luca and R. Merletti. Surface myoelectric signal cross-talk among muscles of the leg. *Electroencephalography and Clinical Neurophysiology*, 69(6):568–575, 1988.

[21] Jeffrey R. Cram, Glenn S. Kasman, and Jonathan Holtz. *Introduction to Surface Electromyography*. Aspen Publication, Gaithersburg, Maryland, 1st edition, 1998.

[22] D. Staudenmann, K. Roeleveld, D. F. Stegeman, and J. H. van Dieen. Methodological aspects of semg recordings for force estimation–a tutorial and review. *Journal of Electromyography and Kinesiology*, 20(3):375–87, 2010.

[23] J. R. Potvin and S. H. M. Brown. Less is more: high pass filtering, to remove up to 99emg signal power, improves emg-based biceps brachii muscle force estimates. *Journal of Electromyography and Kinesiology*, 14(3):389–399, 2004.

[24] J. Perry and G. A. Bekey. Emg-force relationships in skeletal muscle. *Crit Rev Biomed Eng*, 7(1):1–22, 1981.

[25] Mervin Chandrapal, XiaoQi Chen, WenHui Wang, Benjamin Stanke, and Nicolas Le Pape. Investigating improvements to neural network based emg to joint torque estimation. *Paladyn. Journal of Behavioral Robotics*, 2(4):185–192, 2011. 10.2478/s13230-012-0007-2.

[26] Jer-Junn Luh, Gwo-Ching Chang, Cheng-Kung Cheng, Jin-Shin Lai, and Te-Son Kuo. Isokinetic elbow joint torques estimation from surface emg and joint kinematic data: using an artificial neural network model. *Journal of Electromyography and Kinesiology*, 9(3):173–183, 1999.

[27] H. S. Milner-Brown and R. B. Stein. The relation between the surface electromyogram and muscular force. *Journal of Physiology*, 246:549–69, 1975.

[28] Carlo J. De Luca. The use of surface electromyography in biomechanics. *Journal of Applied Biomechanics*, 13(2):135–163, 1997.

[29] J. R. Potvin, R. W. Norman, and S. M. McGill. Mechanically corrected emg for the continuous estimation of erector spinae muscle loading during repetitive lifting. *European Journal of Applied Physiology and Occupational Physiology*, 74(1-2):119–32, 1996.

[30] J. R. Potvin, S. Brown, J. Dowling, and S. Tolmie. High pass filtering beyond 100 hz improves surface emg-based force predictions for the biceps brachii. *Archives of Physiology and Biochemistry*, 108(1-2):156–156, 2000.

[31] John Henry Holland. *Adaptation in natural and artificial systems: an introductory analysis with applications to biology, control, and artificial intelligence*. Bradford Books. MIT Press, 1992.

[32] Kenneth V. Price, Rainer M. Storn, and Jouni A. Lampinen. *Differential Evolution: A Practical Approach to Global Optimization*. Springer, Berlin, 2005.

[33] W.D. McArdle, F.I. Katch, and V.L. Katch. *Exercise Physiology: Energy, Nutrition, and Human Performance*. Exercise Physiology (MC Ardle) Series. Lippincott Williams & Wilkins, 2007.

[34] Beth Morgan, Sarah J. Woodruff, and Peter M. Tiidus. Aerobic energy expenditure during recreational weight training in females and males. *Journal of Sports Science and Medicine*, 2:117–122, 2003.

INTECH